Degradation Behavior of Lithium-Ion Batteries during Calendar Ageing – The Case of the Internal Resistance Increase

Stroe, Daniel-Ioan; Swierczynski, Maciej Jozef; Kær, Søren Knudsen; Teodorescu, Remus

Published in:
I E E E Transactions on Industry Applications

DOI (link to publication from Publisher):
10.1109/TIA.2017.2756026

Publication date:
2018

Document Version
Accepted author manuscript, peer reviewed version

Degradation Behavior of Lithium-Ion Batteries during Calendar Ageing – The Case of the Internal Resistance Increase

Daniel-Ioan Stroe, Maciej Swierczynski, Søren Knudsen Kær, Remus Teodorescu
Department of Energy Technology
Aalborg University
Aalborg, Denmark
dis@et.aau.dk

***Abstract*—Lithium-ion batteries are regarded as the key energy storage technology for both e-mobility and stationary renewable energy storage applications. Nevertheless, Lithium-ion batteries are complex energy storage devices, which are characterized by a complex degradation behavior, which affects both their capacity and internal resistance. This paper investigates, based on extended laboratory calendar ageing tests, the degradation of the internal resistance of a Lithium-ion battery. The dependence of the internal resistance increase on the temperature and state-of-charge level have been extensive studied and quantified. Based on the obtained laboratory results, an accurate semi-empirical lifetime model, which is able to predict with high accuracy the internal resistance increase of the Lithium-ion battery over a wide temperature range and for all state-of-charge levels was proposed and validated.**

Keywords—Lithium-Ion Battery, Internal Resistance, Degradation, Calendar Ageing, Modelling.

I. INTRODUCTION

Among the available ES technologies, Lithium-ion (Li-ion) batteries have detached as one of the very few solutions, which are able to successfully meet the requirements imposed by both electricity grids and transportation sectors [1], [2]. This has become possible thanks to recent developments of Lithium batteries based on new and/or improved materials, which have resulted in batteries with high performance (e.g., high gravimetric and volumetric energy density, reduced self-discharge etc.), long calendar and cycle lifetime, and increased safety [3], [4]. Nevertheless, even though their cost is expected to lower in the future, the major issue, which prevents at the moment a faster widespread use of Lithium-based batteries in the aforementioned sectors, is their high cost combined with performance and degradation uncertainties [5].

A solution to mitigate these issues is to relay on accurate models which are able to predict accurately the performance and lifetime of the Li-ion batteries. Thus, by having access to accurate models, researchers and end-users of Li-ion batteries are able to assess the economic viability and technical suitability of the battery for a certain application [6], [7], [8]. Consequently, by using battery models, expensive and time demanding field trials can be minimized. Li-ion battery performance models are used to predict mainly the short-term dynamic behavior (e.g., voltage, power etc.) at different conditions (e.g., temperature, load current, state-of-charge (SOC)) [9], [10]. The battery lifetime models are used to estimate the long-term degradation behaviour of the Li-ion battery performance parameters (e.g., capacity, internal resistance etc.) during ageing (both calendar and cycle ageing) [11] – [13]. Even though both type of models are equally important, this research focuses on developing a lifetime model, which is able to predict the internal resistance of Li-ion batteries during calendar ageing.

The internal resistance of Li-ion batteries is a highly important parameter since it is used to determine the batteries' power capability. Consequently, by having accurate information about the degradation behavior of the Li-ion battery internal resistance, and subsequently of the power capability, battery packs and systems can be optimally sized and designed to meet the requirements of the application. Moreover, accurate information about the degradation behavior of the Li-ion battery internal resistance are necessary in order to define and choose the optimal battery cooling system strategy. Lastly, accurate information regarding the internal resistance increase during ageing of the Li-ion battery can be used to define optimal energy management strategies, which will efficiently use the Li-ion battery by maximizing lifetime and reducing safety concerns.

This paper studies the degradation behavior of the internal resistance (i.e., the internal resistance increase) of a certain Li-ion battery chemistry (i.e., lithium iron phosphate – LFP) during calendar ageing at different temperature and SOC levels. The evolution of the internal resistance during cycle ageing for the same Li-ion battery chemistry was briefly investigated in [14], while in a previous work we have evaluated its evolution during one year storage at different elevated temperatures [15]. Nevertheless, most of the available degradation studies on the lithium iron phosphate-based batteries are not focused on the internal resistance but on other performance parameters such as capacity and AC impedance [11], [13], [16].

In order to perform this study, fifteen identical Li-ion battery cells were aged for a period varying between 24 and 36 months and the internal resistance increase and its dependence on the storage time, temperature and SOC-level was quantified. Based on the obtained results, a lifetime model which is able to estimate the internal resistance increase during calendar ageing was developed, parameterized, and successfully validated.

II. State-of-the-Art

The ageing of Li-ion batteries is a complex combination of a large number of electrochemical and mechanical processes, which are highly influenced by the operating conditions [17], [18]. The capacity fade and resistance increase (and subsequently power fade) do not originate from one single cause but from various ageing mechanism and their possible interactions [17]. Furthermore, the aforementioned performance parameters degrade during both calendar and cycling ageing [17], [18]. Even though the ageing mechanism at the two electrodes depend on the choice of the electrode material, there are similarities between different electrode materials [19].

Usually the ageing mechanism that occur at the anode and cathode are significantly different [17] and are briefly discussed in the followings. Graphite is mainly used as an anode material in Li-ion batteries; this is also the case of the Li-ion battery which is studied in this paper. The most common ageing mechanism that takes place at the anode and cause the increase of the internal resistance (and subsequently power fade) is the solid electrolyte interface (SEI) formation and growth [17] – [19]; furthermore, the formation and growth of the SEI results into a progressive contact loss within the composite anode, which will cause additional increase of the resistance of the battery cell [17], [19]. According to [17] and [18], the electrolyte decomposition and the SEI formation are enhanced by operating the battery at high temperatures and high SOC-levels; this is in good agreement with the results presented in [20] for a LFP-based battery, which shows a fast internal resistance increase when stored at high SOCs and temperatures. An additional ageing mechanisms, which causes the increase of the battery's resistance, is the corrosion of the current collectors [17]; this process is mainly driven by the battery operation at low SOCs.

The internal resistance increase is also influenced by the ageing mechanisms that occur at the battery's cathode. Binder decomposition, oxidation of the conductive agent, and corrosion of the current collector at the positive electrode lead to reduced conductivity between particles and consequently resistance increase [17] – [19]. As illustrated in [18], these mechanisms are mainly enhanced by storage of the Li-ion batteries at high temperatures. Moreover, the internal resistance increase is caused also by the electrolyte decomposition, which results into a surface layer formation at the cathode side [17], [18].

Different particularities regarding the evolution of the Lithium-ion battery's internal resistance during ageing have already been presented in the literature in different studies.

Most of these studies were carried out considering various cycle ageing conditions [12], [21] – [26] or different driving profiles [27], [28]. Furthermore, the aforementioned cycle ageing studies have been performed for different Li-ion battery chemistries, as follows. The variation of the internal resistance with the depth-of-discharge for fresh and aged (after 100 cycles) LFP-based Li-ion batteries was analyzed in [21]. For the same Li-ion battery chemistry, the internal resistance increase due to cycle ageing at 50°C was studied in [23]; the internal resistance was measured after 600 full cycles at four different temperatures and current pulse lengths, showing a substantial increase with the cycle number and temperature decrease and only a slight increase with the pulse duration [23]. The evolution of the internal resistance of a NMC-based Li-ion battery during cycling ageing was investigated in depth for various SOC levels, temperatures, and currents by Waag et al. in [22]. The effect of the cycling temperature on the resistance increase rate was evaluated by Feng et al. in [26] for an LCO-based battery; using an electrochemistry-based model, the authors have observed, during 250 cycles, an increase of the total resistance of electrodes resistance and electrode/electrolyte resistance of 33.64% and 93.29%, when the batteries were cycled at 25°C and 55°C, respectively. Semi-empirical models, which are able to estimate the internal resistance increase during cycle ageing at various conditions were developed for $LiNiCoO_2$-based and NMC-based Lithium-ion batteries in [24] and [12], respectively.

The second group of studies have focused on analyzing the increase of the internal resistance during calendar ageing [29] – [33]. Thus, Matsushima et al. have analyzed the evolution of the internal resistance during trickle-charge at high voltage levels (i.e., higher than 4 Volts) and increased temperature levels (i.e., above 45°C) [29]; the authors found out that for the same idling temperature, the internal resistance increase was quasi-independent on the charge voltage. A statistical methodology for predicting the internal resistance increase of Li-ion batteries (no chemistry specified) during calendar ageing was proposed in [30]. Furthermore, lifetime models, which are able to estimate the internal resistance increase during storage at different temperatures and SOC-levels were developed in [31] (for the $LiNiCoO_2$ chemistry) and [32] (for the NMC chemistry). Schmalstieg et al. have observed a linear dependence on the storage voltage and an exponential dependence on the storage temperature of the internal resistance increase rate [32]. None of the aforementioned studies have been focused on assessing and modeling the internal resistance increase of a Li-ion battery based on the LFP chemistry. Thus, in this work, we propose an accurate lifetime model, which is able to estimate the degradation of the internal resistance of a LFP-based Li-ion battery. The proposed model is based on accelerated ageing experiments carried out over a period of at least 24 months.

III. Experimental Set-Up

A. Lithium-Ion Battery Under Test

The Li-ion battery family is broad, with many chemistries being commercialized at present [34]. Nevertheless, for this research, Li-ion batteries based on the lithium iron phosphate ($LiFePO_4$) chemistry were used; because they use lithium iron phosphate at the cathode and graphite carbon at the anode, as

active materials, they are further referred to as LFP/C-based Li-ion batteries. All the tests presented in this research were performed on cylindrical LFP/C battery cells (type 26650) with a nominal capacity of 2.5 Ah and a nominal voltage of 3.3 V.

B. *Accelerated Calendar Ageing*

The lifetime of the LFP/C-based battery cells, which were considered in this work, is in the range of years, as shown in [11], [35]. Therefore, in order to obtain the desired information about the degradation behaviour of their internal resistance in a relatively reduced time, the battery cells were subjected to an accelerated calendar ageing procedure, similar to the one presented in [13]. The main stress factor used for accelerating the ageing of the battery cells was the high temperature. Besides the temperature, the second stress factor, which affects the calendar lifetime of the Li-ion batteries is the state-of-charge at which they are stored [11], [16]. As presented in the already published literature, the degradation of the Li-ion battery cells performance parameters (e.g., internal resistance) varies non-linearly with the stress levels [12], [13]. Thus, to be able to accurately extrapolate the degradation of the LFP/C battery cells at a temperature, which maximizes the lifetime (e.g., 25°C – for stationary applications), and to interpolate between the storage SOC levels (to obtain the degradation over the entire SOC interval), three stress levels were considered for both stress factors. Consequently, LFP/C battery cells were subjected to accelerated ageing tests at five conditions, as summarized in Table I. During the accelerated calendar ageing tests, the battery cells were stored, at open-circuit condition, in climatic chambers, in order to obtain the desired temperature levels (see Fig. 1); the relative humidity inside the climatic chambers was approximately 41%.

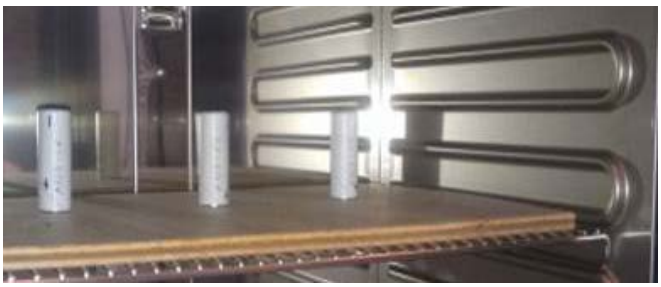

Fig. 1. LFP/C battery cells during accelerated calendar ageing tests.

TABLE I. ACCELERATED AGEING TEST CONDITIONS

Ageing Case	Temperature	SOC
Case 1	55°C / 328 K	50%
Case 2	47.5°C / 320.5 K	50%
Case 3	40°C / 313 K	50%
Case 4	55°C / 328 K	10%
Case 5	55°C / 328 K	90%

After 30 days of storage at the conditions presented in Table I, the LFP/C battery cells were subjected to a reference performance test (RPT) sequence. During the RPT, among various performance parameters, the internal resistance of the battery cells was measured in order to quantify its degradation trend. Afterwards, the accelerated calendar ageing test were resumed for another 30 days and for the corresponding RPT. This procedure was repeated for a period of 24 or 36 months depending on the ageing test case.

C. *Internal Resistance Measurement*

During each RPT, the internal resistance of the LFP/C battery cells was measured at 25°C (i.e., 298 K) using the current pulse train shown in Fig. 2; the internal resistance was measured for both charging and discharging current pulses and for four C-rates (i.e., 4C, 2C, 1C, and 0.5C), since the value of the resistance changes significantly with the amplitude of the load current. Each current pulse was applied for 18 seconds [36], while prior to the pulse a 15 minutes relaxation period was imposed in order to allow the LFP/C cell to reach thermodynamic stability. Because the value of the internal resistance of Li-ion batteries depends on the SOC and different internal resistance degradation trends might be obtained depending on the SOC at which the resistance is measured, the current pulse train was applied during each RPT at three SOC levels (i.e., 20%, 50%, 80% SOC) as presented in Fig. 3.

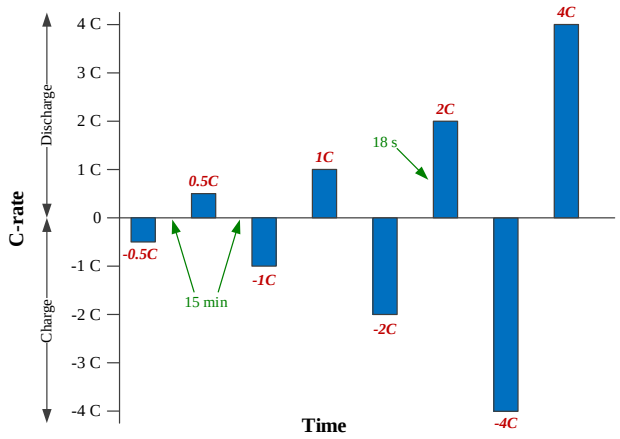

Fig. 2. Current pulse train used to measure the internal resistance of the tested LFP/C battery cells; where 1C equals a current with the amplitude of 2.5A.

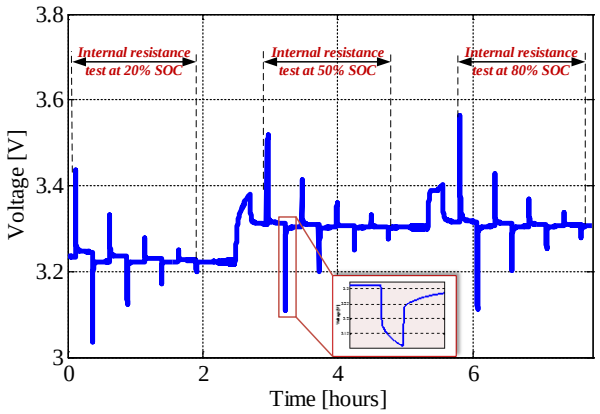

Fig. 3. LFP/C battery cell voltage response during internal resistance measurement at 20%, 50%, and 80% SOC with the pulse profile presented in Fig. 2.

IV. Results

For each of the five accelerated calendar ageing cases, which are summarized in Table I, three LFP/C battery cells were considered in order to ensure consistency of the obtained ageing results and to eliminate possible outliers. Thus, the internal resistance values and the degradation trends presented hereafter represent the average over the three values obtained for the three cells corresponding to each case. The battery cells' internal resistance was computed based on Ohm's law, as shown in Fig. 4. The effect of the internal resistance degradation on the battery voltage response during a 4C discharge current pulse is presented in Fig. 5 for one of the considered ageing cases.

As it was mentioned in the previous section, the internal resistance of the cells was measured at three SOC levels; however, in this work, only the internal resistance values (and corresponding trends) measured at 80% SOC during a discharging current pulse were considered for the degradation analysis. For determining the degradation trends of the internal resistance, which were caused by ageing at various conditions (see Table I), the internal resistance values measured at different ageing levels were linked to the values measured at the cells' beginning-of-life (BOL) according to (1).

$$R_{i,increase}\,[\%] = (R_{i,present} - R_{i,BOL}) / R_{i,BOL} \cdot 100\% \qquad (1)$$

where, $R_{i,increase}$ represents the internal resistance increase of the LFP/C cell (expressed in per cent), $R_{i,present}$ represents the internal resistance measured after each RPT (expressed in Ohms), and $R_{i,BOL}$ represents the internal resistance measured at the cell's BOL (expressed in Ohms).

As illustrated in Fig. 6, the internal resistance of the studied LFP/C battery cell has increased with the storage time and its degradation behaviour is accelerated by increasing the storage temperature (left column), and the storage SOC (right column); even though the internal resistance of the battery cells was measured after each 30 days of calendar ageing, the evolution of the internal resistance is presented with a resolution of 120 days, for clarity purposes. Furthermore, the ageing trends of the internal resistance, which were observed and are presented in Fig. 6, are only slightly dependent on the C-rate. Thus, only the ageing results for a 4C-rate will be further analyzed and used for building the cell's lifetime model. The influence of the storage temperature and SOC level on the internal resistance increase for the case when the internal resistance was measured at 80% SOC during a 4C discharging current pulse are discussed in the next section.

V. Internal Resistance Lifetime Model

To analyze the internal resistance increase behavior of the tested LFP/C battery cells, a two steps fitting procedure was followed. Firstly, the dependence of the internal resistance increase on the storage time was obtained for each considered ageing case. Secondly, the dependence on the storage temperature and SOC-level was determined. All the fitting processes were performed using the Curve Fitting Toolbox from MATLAB® considering a nonlinear least squares method; the quality of the fitting was evaluated using the coefficient of determination R^2. For all the fitting processes, we have used the internal resistance values measured after each 30 days of calendar ageing.

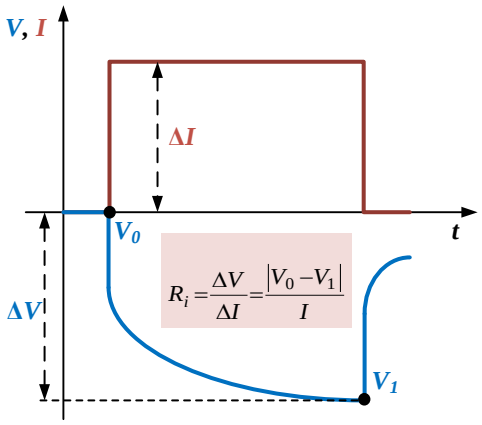

Fig. 4. Theoretical battery cell voltage response (blue) during an 18 seconds discharging current pulse (red).

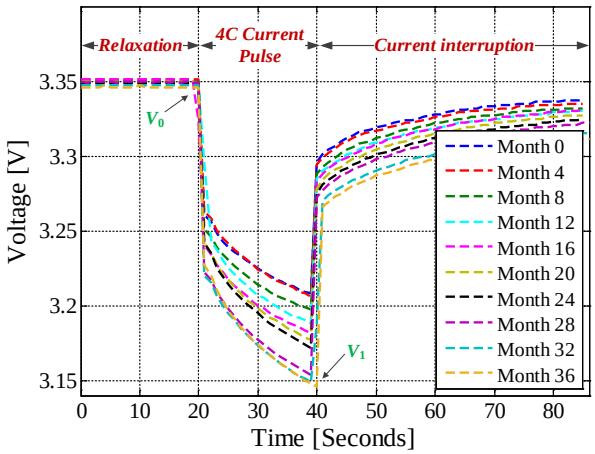

Fig. 5. Voltage response during a 4C discharge pulse at different degradation lev els of the LFP/C battery cells (*Case1* aging condition).

$$R^2 = 1 - \frac{SS_{res}}{SS_{tot}} = \frac{\sum_{i=1}^{n}(y_i - f_i)^2}{\sum_{i=1}^{n}(y_i - \bar{y})^2} \qquad (2)$$

where, SS_{res} represents the sum of squares of residuals (deviation between the measured points and the fitted curve) and SS_{tot} represents the total sum of squares (deviation between the measured points and their average value).

A. Dependence on storage time

Initially, five different functions (i.e., linear, logarithmic, square-root, power law, and power law with fixed exponent) were evaluated for fitting the internal resistance increase during calendar ageing. Based on the obtained results, the power law function give in (3) was selected for fitting the measured

degradation behavior of the internal resistance at the five considered calendar ageing conditions.

$$R_{i,increase}(t) = a_t \cdot t^{0.8} \quad (3)$$

where, a_t represents the coefficient of the power law function and t represents the storage time expressed in months.

The obtained fitting functions for each of the five ageing cases and the corresponding R^2 values are summarized in Table II. Based on the obtained values for the coefficient of determination R^2 (see Table II), it was concluded that the fitting function (3) is able to estimate accurately the increase of the internal resistance during calendar ageing at different conditions.

TABLE II. DEPENDENCE OF THE INTERNAL RESISTANCE INCREASE ON THE STORAGE TIME

Ageing Case	Fitting function	Accuracy
Case 1	$4.217 \cdot t^{0.8}$	0.979
Case 2	$2.607 \cdot t^{0.8}$	0.966
Case 3	$2.117 \cdot t^{0.8}$	0.961
Case 4	$2.974 \cdot t^{0.8}$	0.994
Case 5	$5.182 \cdot t^{0.8}$	0.942

B. Dependence on the storage temperature

The measured and fitted internal resistance increase trends for the LFP/C cells, which were aged at 50% SOC and three temperatures (i.e., Case 1, Case 2, and Case 3) are shown in Fig. 7. The a_t fitting coefficients, corresponding to the three aforementioned calendar ageing cases, were used to determine the dependence of the internal resistance increase on the temperature, during the second step of the two-steps fitting procedure. As illustrated in Fig. 8, an exponential function was found to express accurately (R^2 = 0.963) the relationship between the temperature fitting coefficients and the storage temperature. This exponential dependence is in good agreement with Arrhenius' law, which predicts a doubling of the reaction rate (in this case, internal resistance increase) for a 10°C increase in temperature. By combining the power law function (3), which expresses the dependence of the resistance increase on the storage time, with the exponential dependence of the resistance increase on the temperature, a model that is able to estimate the internal resistance increase during storage at 50% SOC and different temperatures (mainly higher than 25°C (i.e., 298 K)), was obtained:

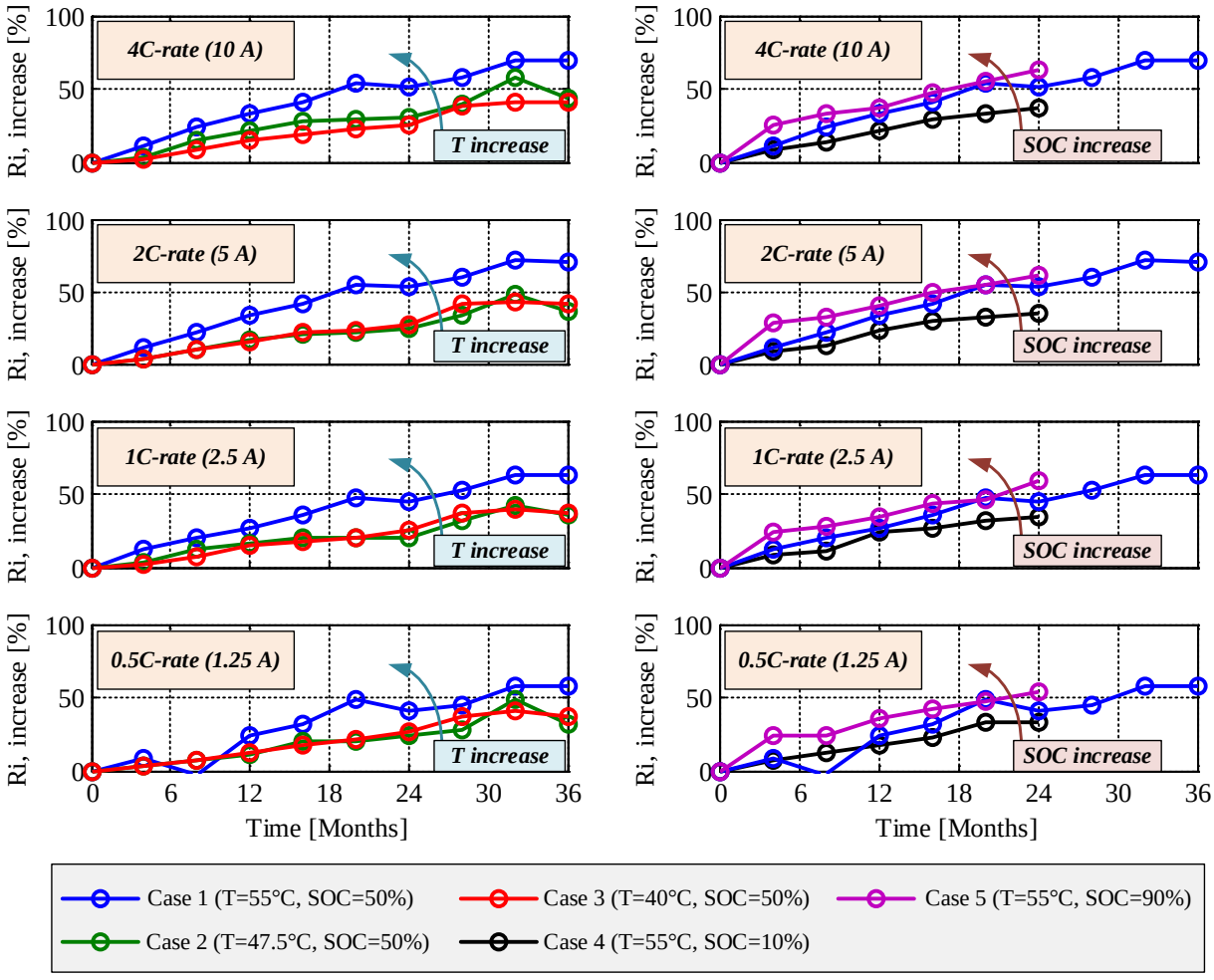

Fig. 6. Internal resistance increase measured for various C-rates and its dependence on storage temperature (left) and storage SOC level (right).

$$R_{i,increase}\,(t,T) = 2.883\cdot10^{-7}\cdot e^{0.05022\cdot T}\cdot t^{0.8} \quad (4)$$

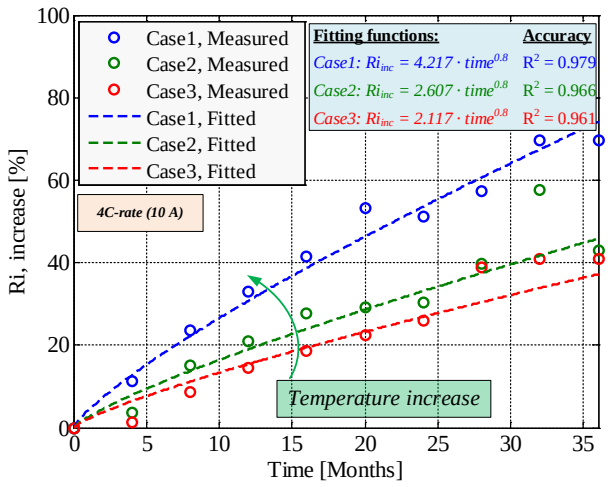

Fig. 7. Dependence on storage temperature of the internal resistance increase measured on LFP/C battery cells aged at 50% SOC

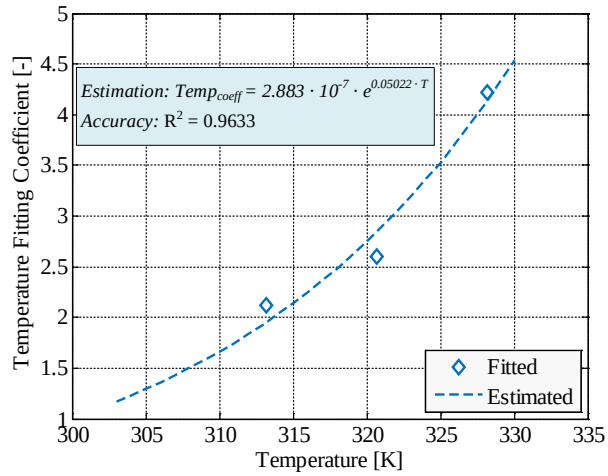

Fig. 8. Exponential relationship between the obtained curve fitting coefficients and the considered storage temperature

C. *Dependence on the storage SOC-level*

During the second step of the fitting procedure, the dependence of the internal resistance increase on the SOC-level, at which the LFP/C cells were stored, was investigated too. The measured and fitted internal resistance trends of the LFP/C battery cells, which were stored at 55°C (i.e., 328 K) and three SOC-levels are illustrated in Fig. 9. Similarly to the previous case, it was found out that the internal resistance was increasing exponentially with increasing the storage SOC-level; this dependence is graphically illustrated in Fig. 10. Based on the power law (3) and the relationship presented in Fig. 10, a model, which is able to estimate the increase of the LFP/C cells' resistance during storage at 55°C (i.e., 328 K) and over the whole SOC interval, was obtained:

$$R_{i,increase}\,(t,SOC) = 2.897\cdot e^{0.006614\cdot SOC}\cdot t^{0.8} \quad (5)$$

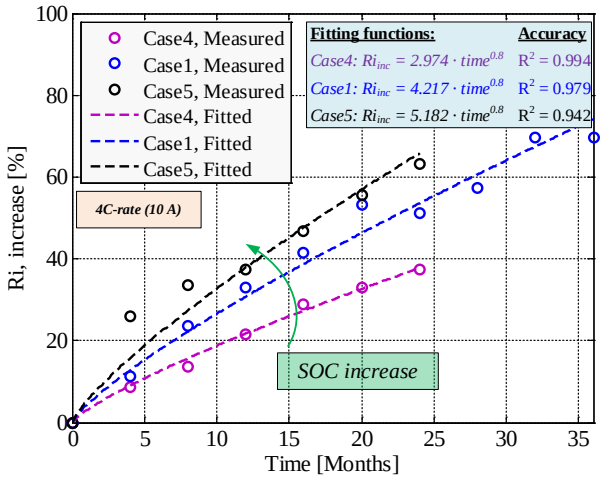

Fig. 9. Dependence on storage SOC-level of the internal resistance increase measured on LFP/C battery cells aged at 55°C.

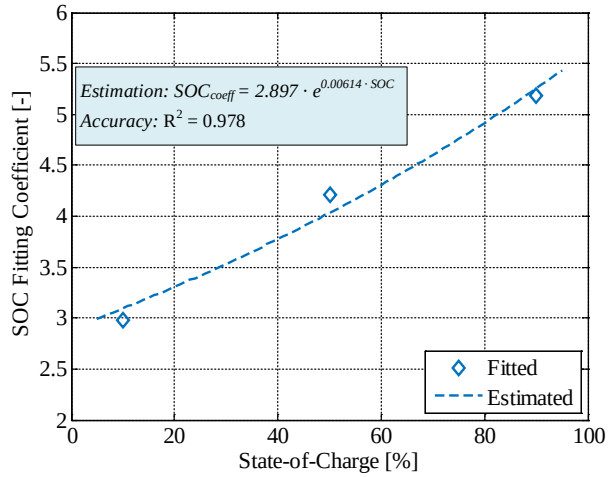

Fig. 10. Exponential relationship between the obtained curve fitting coefficients and the considered storage SOC level.

As described until this point, the dependence of the internal resistance increase on the storage temperature and on the storage SOC-level were fitted separately, as given in (4) and (5), respectively. Thus, it was assumed that the effect of temperature on the internal resistance increase, which was measured and modeled for a 50% SOC (given in (4)), is the same at any other SOC. Similarly, we assumed that the effect of SOC on the internal resistance increase, which was measured and modeled for a temperature of 55°C (given in (5)), is the same at any other temperature. In order to obtain a function, which connects the aforementioned dependences into

a single figure of merit, a scaling of the two functions was used. Since possible interactions between the storage temperature and the storage SOC level were neglected, a scaling process of the two models (i.e., (4) and (5)) was considered accurate enough. These two models had one ageing case in common (i.e., Case 1 - 55°C, 50% SOC). Thus, we considered that it exists a scaling factor, which when multiplied with (4) for a temperature of 55°C (i.e., 328 K) should return a value equal to 1; the obtained value of the scaling factor is 0.2415. Thus, based on this value of the scaling factor, the developed lifetime model, which is able to predict the increase of the LFP/C battery cells' internal resistance during storage at different conditions (i.e., temperature and SOC) is given in (6). In (4) – (6), the internal resistance increase R_i, is expressed in percent, the SOC is expressed in percent, the time t, is expressed in months, and the temperature T is expressed in degrees Kelvin. Based on the developed lifetime model (6), the increase of the tested battery cells' internal resistance for the temperature interval 25°C – 55°C (i.e., 298 K – 328 K), for the whole SOC interval, and for a storage period of 20 years is presented in Fig. 11. According to the obtained results, during the considered time interval, the internal resistance of the tested LFP/C battery cells will increase by 71% if stored at 50% SOC and 25°C; furthermore, for an increase of the storage SOC from 50% to 100%, a doubling of the initial internal resistance will be obtained.

VI. Validation of the Lifetime Model

In order to verify the developed internal resistance increase lifetime model and to determine its accuracy, an additional calendar ageing tests was performed. During this test, the LFP/C battery cells were stored at open circuit voltage conditions at 45°C (i.e., 318 K) and 70% SOC. A comparison between the internal resistance increase measured during the validation test and the predicted internal resistance increase for similar ageing conditions is presented in Fig. 12. As shown in Fig. 12, the developed model has the tendency to slightly overestimate the increase of the internal resistance; nevertheless, during the considered 24 months of validation testing period, the maximum absolute error, computed based on (7), did not exceed 3.1% of internal resistance increase. Moreover, the average relative estimation error for the same period, computed based on (8), was 9.72%.

$$\epsilon_{abs\_max} = \max\left(\left|R_{increase\ ,meas}(i) - R_{increase\ ,estim}(i)\right|\right) \quad (7)$$

$$\overline{\epsilon_r} = 100 \cdot \left|\frac{R_{increase\ ,meas} - R_{increase\ ,estim}}{R_{increase\ ,meas}}\right| \quad (8)$$

VII. Concluions

This paper has investigated the degradation behavior of LFP/C battery cells in terms of internal resistance increase during calendar ageing. For performing this investigation, five different accelerated calendar ageing tests were carried out and data about the internal resistance increase of the LFP/C battery cells were collected for a period which varied between 24 and 36 months, depending on the considering ageing case. By analyzing the data obtained from measurement it was find out that the internal resistance is increasing non-linearly during calendar ageing following a power law function. Furthermore, the increase of the internal resistance of the tested LFP/C battery cells is accelerated exponentially by increasing the storage temperature and by increasing the storage SOC-level. Furthermore, based on the obtained internal resistance ageing trends, a lifetime model, which is able to predict the internal resistance increase at various temperatures and SOC-levels was developed and parameterized. By performing an additional calendar ageing tests, the proposed lifetime model was verified showing a high estimation accuracy.

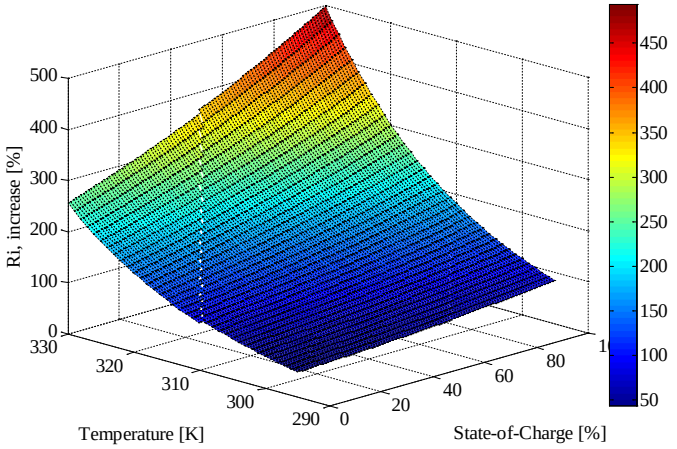

Fig. 11. Estimation of the internal resistance increase for LFP/C battery cells stored at different temperature and SOC levels during a period of 20 years.

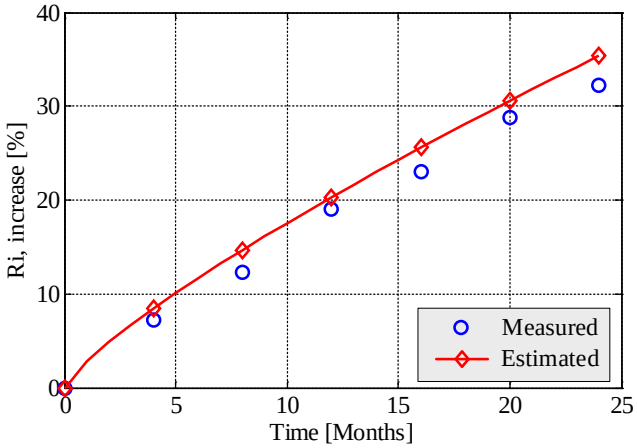

Fig. 12. Comparison between measured and estimated internal resistance increase of the LFP/C battery cells.

$$R_{i,increase}(t,T,SOC) = (6.9656 \cdot 10^{-8} \cdot e^{0.05022 \cdot T}) \cdot (2.897 \cdot e^{0.006614 \cdot SOC}) \cdot t^{0.8} \quad (6)$$

REFERENCES

[1] B. Dunn, H. Kamath, and J.-M. Tarascon, "Electrical energy storage for the grid: A battery of choices," *Science*, vol. 334, pp. 928–935, 2011.

[2] S. Vazquez, S.M. Lukic, E. Galvan, L.G. Franquelo, J.M. Carrasco, "Energy Storage Systems for Transport and Grid Applications," IEEE Transactions on Industrial Electronics, vol. 57, no.12, pp. 3881-3895, 2010.

[3] DOE/EPRI 2013 Electricity Storage Handbook in Collaboration with NRECA, Tech. Rep. SAND2013-5131, Sandia National Laboratories, 2013.

[4] J.B. Goodenough and K.-S. Park, "The Li-Ion Rechargeable Battery: A Perspective," Journal of the American Chemical Society, vol. 135, no. 4, pp. 1167-1176, 2013.

[5] I. Gyuk et al., "Grid Energy Storage", US Department of Energy, December 2013.

[6] M. Swierczynski, D.-I. Stroe, A.I. Stan, R. Teodorescu, "Lifetime and economic analyses of lithium-ion batteries for balancing wind power forecast error," International Journal of Energy Research, vol. 39, no. 6, pp. 760-770, May 2015.

[7] J. W. Lee, S.W. Kim, Y.H. Song, S. Kim, T.T. Yoon, "Economic benefit of energy storage system for frequency regulation," IEEE Power and Energy Conference at Illinois (PECI), pp. 1-5, 2016.

[8] J. Fleer, S. Zurmühlen, J. Badeda, P. Stenzel, J. Hake, D. U. Sauer, "Model-based economic assessment of stationary battery systems providing primary control reserve," 10th International Renewable Energy Storage Conference – IRES 2016, Düsseldorf, Germany.

[9] A. Hentunen, T. Lehmuspelto, J. Suomela, "Time-Domain Parameter Extraction Method for Thévenin-Equivalent Circuit Battery Models," IEEE Transactions on Energy Conversion, vol. 29, no. 3, pp. 558-566, September 2014.

[10] M. Chen and G.A. Rincon-Mora, "Accurate electrical battery model capable of predicting runtime and I-V performance," IEEE Transactions on Energy Conversion, vol. 21, no. 2, pp. 504-511, June 2006.

[11] M. Swierczynski, D.-I. Stroe, A.I. Stan, R. Teodorescu, S.K. Kær, "Lifetime Estimation of the Nanophosphate LiFePO4/C Battery Chemistry Used in Fully Electric Vehicles," IEEE Transactions on Industry Applications, vol. 51, no. 4, pp. 3453-3461, July 2015.

[12] M. Ecker et al., "Development of a lifetime prediction model for lithium-ion batteries based on extended accelerated aging test data," Journal of Power Sources, vol. 215, pp. 248-257, 2012.

[13] D.-I. Stroe, M. Swierczynski, A.-I. Stan, R. Teodorescu, S.J. Andreasen, "Accelerated Lifetime Testing Methodology for Lifetime Estimation of Lithium-Ion Batteries Used in Augmented Wind Power Plants," IEEE Transactions on Industry Applications, vol.50, no.6, pp.4006-4017, 2014.

[14] Y. Zhang, C.-Y. Wang, X. Tang, "Cycling degradation of an automotive $LiFePO_4$ lithium-ion battery," Journal of Power Sources, vol. 196, pp. 1513-1520, 2011.

[15] D.-I. Stroe, M. Swierczynski, A.-I. Stan, R. Teodorescu, S.J. Andreasen, "Experimental investigation on the internal resistance of Lithium iron phosphate battery cells during calendar ageing," IEEE Industrial Electronics Conference IECON 2013, pp. 6734-6739, 2013.

[16] M. Kassem, J. Bernard, R. Revel, S. Pelissier, F. Duclaud, C. Delacourt, "Calendar aging of graphite/LiFePO4 cell," Journal of Power Sources, vol. 208, pp. 296-305, 2012.

[17] J. Vetter et al., "Ageing mechanims in lithium-ion batteries," Journal of Power Sources, vol. 147, pp. 269-281, 2005.

[18] M. Brouselly et al, "Main aging mechanisms in Li ion batteries," Journal of Power Sources, vol. 146, pp. 90-96, 2005.

[19] J. Groot, "State-of-Health Estimation of Li-ion Batteries: Ageing Models," Ph.D. Thesis, Chalmers University of Technology, Sweden, 2014.

[20] E. Sarasketa-Zabal, I. Gandiga, L.M. Rodriguez-Martinez, I. Villarreal, "Calendar ageing analysis of a LiFePO4/graphite cell with dynamic model validations: Towards realistic lifetime predictions," Journal of Power Sources, vol. 272, pp. 45-57, 2014.

[21] J. Shim and K. A. Striebel, "Cycling performance of low-cost lithium ion batteries with natural graphite and LiFePO4," Journal of Power Sources, vol. 119-121, pp. 955-958, 2003.

[22] W. Waag, S. Käbitz, D. U. Sauer, "Experimental investigation of the lithium-ion battery impedance characteristic at various conditions and aging states and its influence on the application," Applied Energy, vol. 102, pp. 885-897, 2013.

[23] Y. Zhang, C.-Y. Wang, X. Tang, "Cycling degradation of an automotive LiFePO4 lithium-ion battery," Journal of Power Sources, vol. 196, pp. 1513-1520, 2011.

[24] I. Bloom et al., "Mechanisms of impedance rise in high-power, lithium-ion cells," Journal of Power Sources, vol. 111, pp. 152-159, 2002.

[25] B. V. Ratnakumar, M. C. Smart, L. D. Whitcanack, R. C. Ewell, "The impedance characteristics of Mars Exploration Rover Li-ion batteries," Journal of Power Sources, vol. 159, pp. 1428-1439, 2006.

[26] F. Leng, C. M. Tan, M. Pecht, "Effect of Temperature on the Aging rate of Li Ion Battery Operating above Room Temperature," Scientific Reports, vol 5:12967, 2015.

[27] R. B. Wright et al., " Power fade and capacity fade resulting from cycle-life testing of Advanced Technology Development Program lithium-ion batteries," Journal of Power Sources, vol. 119-121, pp. 865-869, 2003.

[28] J. Nadeau, M. R. Dubois, A. Descrochers, N. Denis, "Ageing estimation of lithium-ion batteries applied to a three-wheel PHEV roadster," IEEE 2013 IEEE Vehicle Power and Propulsion Conference (VPPC), pp. 1-6, 2013.

[29] T. Matsushima, S. Yakagi, S. Muroyama, T. Horie, "Lifetime and residual capacity estimate for Lithium-ion secondary cells for stationary use in telecommunications systems," IEEE, INTELEC 05 - Twenty-Seventh International Telecommunications Conference, pp. 199-204, 2005.

[30] E. V. Thomas, I. Bloom, J. P. Christophersen, V. S. Battaglia, "Statistical methodology for predicting the life of lithium-ion cells via accelerated degradation testing," Journal of Power Sources, vol. 184, pp. 312-317, 2008.

[31] R. B. Wright et al., "Calendar- and cycle-life studies of advanced technology development program generation 1 lithium-ion batteries," Journal of Power Sources, vol. 110, pp. 445-470, 2002.

[32] J. Schmalstieg, S. Käbitz, M. Ecker, D. U. Sauer, "A holistic aging model for $Li(NiMnCo)O_2$ based 18650 lithium-ion batteries," Journal of Power Sources, vol 257, pp. 325-334, 2014.

[33] D.-I. Stroe, M. Swierczynski, S. K. Kær, R. Teodorescu, "A comprehensive study on the degradation of lithium-ion batteries during calendar ageing: The internal resistance increase," in Proc. 2016 IEEE Energy Conversion Congress and Expo. (ECCE), Milwaukee, WI, pp. 1 – 7, DOI: 10.1109/ECCE.2016.7854664.

[34] A.I. Stan, M. Swierczynski, D.-I. Stroe, R. Teodorescu, S.J. Andreasen, "Lithium ion battery chemistries for renewable energy storage to automotive and back-up power applications – An overview," IEEE International Conference on Optimization of Electrical and Electronic Equipment OPTIM 2014, pp. 713-720, 2014

[35] C. Vartanian, N. Bentley, "A123 systems' advanced battery energy storage for renewable integration," 2011 IEE/PES Power Systems Conference and Exposition (PSCE), pp. 1-6, 20-23 March 2011.

[36] ISO 12405-1 Electrically propelled road vehicles – Test specification for lithium-ion traction battery packs and systems – Part 1: High-power applications, 2011;